## MISSION DESIGN FOR THE EXPLORATION OF NEPTUNE AND TRITON

**Stefano Campagnola**(1), **Arnaud Boutonnet**(2), **Waldemar Martens**(3), **and Adam Masters**(4)
(1)*ISAS/JAXA, Yoshinodai 3-1-1, Sagamihara, Kanagawa 252-5210, Japan, +81 70 6912 1162, stefano.campagnola@jaxa.jp*
(4)*ISAS/JAXA, Yoshinodai 3-1-1, Sagamihara, Kanagawa 252-5210, Japan*
(2)*ESOC/ESA, Robert-Bosch-Strasse 5, 64293 Darmstadt, Germany*
(3)*GCI at ESOC/ESA, Robert-Bosch-Strasse 5, 64293 Darmstadt, Germany*

***Abstract:*** *Neptune and its largest moon Triton are essential pieces of the Solar System puzzle. A mission dedicated to their exploration is challenging in terms of communication, power, and mission design; however, it would yield paradigm-changing advances in multiple fields of planetary science. This paper discusses some enabling technologies for an ESA-led orbiter mission, with emphasis on the trajectory design. The work is motivated by the recent call from ESA to define science themes for the next L-class missions, and is in part summarized in the white paper supporting the science case for the exploration of Neptune and Triton. Among the enabling technologies, a Solar Electric Propulsion (SEP) module would be used in the first part of the interplanetary transfer and ejected before approaching Neptune. The dry mass after the separation of the SEP module would vary from 1400 kg to 1900 kg (depending on the propulsion system used for Neptune orbit insertion), which is comparable to the dry mass of planetary orbiters to Jupiter and Saturn, and of the most recent studies for a NASA's Neptune orbiter.*

***Keywords:*** *ESA white paper, L2/L3 mission, Neptune orbiter, Triton flybys.*

## 1. Introduction

In early 2013 ESA invited the scientific community to propose themes for the next decades of large-class missions (L2 and L3). A team of researchers from European, American, and Japanese institutions submitted a white paper on the science case for a mission to Neptune and Triton. The document included an example mission concept, aimed to demonstrate that the proposed science theme can be addressed with technology that is expected to become available within the L2 and L3 time frames (2028 and 2034). We present here the trajectory design for the mission concept and a high-level discussion on its feasibility, which was included in the white paper. We also present details on the example Triton tour, a new search for of the interplanetary transfers, and a preliminary analysis on the gravity losses at Neptune Orbit Insertion (NOI), which suggests the use of a large chemical propulsion system.

The first section of the paper presents a summary of the mission concept, with emphasis on the enabling technologies for an ESA-led mission. Options with high technological readiness level (TRL) are favored, since a main goal of this study is to focus the required research and technology development in the fewest areas. Heritage for the feasibility of a mission to Neptune is provided by the most recent NASA/JPL mission concept study[1], which analyzed several architectures for a NASA-led mission. Other relevant studies include the Outer Solar System Mission[2] , which was proposed for an ESA M-class mission, and NASA Vision Mission Neptune Orbiter with Probes[3].

The second section of the paper presents several interplanetary transfers using chemical or solar-electric propulsion (SEP). Only the SEP options result in a sufficiently large dry mass for a L-class Neptune orbiter. While some trajectories to Neptune can be found in literature (for both chemical propulsion[4, 2, 1] and SEP [5, 6], in this paper we specifically assume an Ariane 5 ECA launch, and use of European technology for the SEP system. We also present a broad search of chemical propulsion options computed using the software SOURCE[7, 8] , and some example SEP options.

The last section presents an example two-year moon tour at Neptune, which demonstrates that all the science questions can be effectively addressed using Triton as a tour engine. The tour includes 55 flybys, and covers a wide range of Neptune orbits and Triton flyby geometries. Another example of Triton tour can be found in [3].

## 2. A mission to Neptune and Triton

Neptune and Triton hold the keys to paradigm-changing advances in multiple fields of planetary science. Neptune had an important role in the formation of the Solar System; Neptune-sized bodies are the most detected class of exoplanets; Neptune's atmosphere is the most active in the Solar System, with a produced heat flux more than twice its solar input; the magnetic environment has a fast reconfiguration, and its origin and structure are unknown. Neptune's largest moon Triton is probably a captured dwarf planet from the Kuiper belt. The plums detected by Voyager 2 (first detected cryvolcanic activity) hint to the existence of a subsurface ocean, and thanks to the interaction with the magnetic field, they might be a source of the plasma in the Neptune system. In addition to Triton, the Neptune system includes other smaller moons and a complex system of rings, which remains largely unexplored. More details on the science case discussed in the white paper can be found in [9].

The scientific case for the exploration of Neptune and Triton is compelling, however, an orbiter mission to Neptune poses multiple technological challenges. This section present an example mission concept with launch in 2028, with a high level discussion on the main enabling technologies for an ESA-led L-class mission.

### 2.1. Payload Options

To address all the diverse scientific themes, a mission to Neptune must include a Neptune-orbiting spacecraft that makes multiple Triton flybys. If equipped with a payload of modern spacecraft instrumentation, such a spacecraft in orbit around Neptune would be more than sufficient to address all themes. Possible additional mission elements are a Neptune atmospheric descent probe, a Triton lander, and additional spacecraft; however, the inclusion of these enhancing elements is likely to be limited by mission cost and technical feasibility, and so they are not considered here. There are similarities between the Neptune orbiter discussed here and the Galileo and Cassini-Huygens missions to Jupiter and to Saturn and Titan, respectively. In both these cases the first spacecraft to orbit each planet lead to/continues to provide a hugely significant, paradigm-changing scientific return. A Neptune orbiter carrying a similar payload of scientific instruments would cover the wide range of Neptune-Triton science themes. Table 1 lists payload options. All modern spacecraft instrumentation included in Table 1 has a high Technology Readiness Level (TRL) and significant flight heritage. All values for instrument mass and power consumption are estimates. Specific

Table 1. Neptune orbiter payload options. All values of instrument mass and power consumption are estimates based on heritage instruments.

| Instrument | Mass (kg) | Power (W) | Heritage |
|---|---|---|---|
| Narrow-angle camera (NAC) | 9.8 | 14 | Mars Express (SRC), New Horizons (LORRI), JUICE (JANUS) |
| Visible-infrared imager (VIR) | 10.1 | 7.5 | New Horizons (Ralph), Mars Express (OMEGA), Rosetta (VIRTIS), BepiColombo (SIMBIO-SYS) |
| Ultraviolet imaging spectrometer (UVIS) | 5 | 12 | BepiColombo (PHEBUS), Mars Express (SPICAM-UV), JUICE (UVS) |
| Accelerometer (ACC) | 3.5 | 3 | GOCE, GRACE, BepiColombo (ISA) |
| Radio science experiment (including ultrastable oscillator) (RSE) | 3.5 | 45.5 | Rosetta (RSI), New Horizons (REX), BepiColombo (MORE), JUICE (3GM) |
| Magnetometer (MAG) | 3.3 | 3 | Cassini (MAG), Double Star (MAG), Rosetta (RPC), BepiColombo (MERMAG), JUICE (J-MAG) |
| Thermal imager (TMI) | 7 | 20 | BepiColombo (MERTIS) |
| Particle package (plasma, neutrals, energetic neutral atoms) (PP) | 23 | 50 | Cassini (CAPS, MIMI), New Horizons (SWAP, PEPSSI), JUICE (PEP) |
| Radio and plasma wave system (RPWS) | 5.7 | 7.1 | Cassini (RPWS), JUICE (RPWI) |
| Dust Analyser (DA) | 3.2 | 8 | Cassini (CDA), Stardust (CIDA) |

measurement requirements for a Neptune orbiter mission are not discussed here, although the measurement ranges of heritage instruments would very likely be appropriate.

Including all these instruments would result in a total payload mass of ˜70 kg, compared to the ˜60 kg value associated with a Neptune orbiter mission architecture previously studied by NASA[1]. Instrument development between now and the L2/L3 timeframe will likely reduce both mass and power consumption. Note that compared to ESA's JUICE mission the instrument radiation shielding requirements are significantly lower for a Neptune orbiter. Table 2 shows how data taken by each instrument included in Table 1 would address the various Neptune-Triton science themes discussed in [9].

## 2.2. Enabling technologies

### Extended Tracking Network capability

A Neptune orbiter mission would use Ka and X bands for data and telemetry. The previous Neptune orbiter study by NASA[1] showed that a Ka-downlink to a single 34-m antenna yields to a data rate of 1-6 kbps at Neptune, which was deemed too slow for returning useful science. A proposed solution was to use the planned extension of the Deep Space Network (DSN) capabilities (four arrayed 34 m antennas).

**Table 2. Matrix relating science themes to payload options.**

| Science theme | NAC | VIR | UVIS | ACC | RSE | MAG | TMI | PP | RPWS | DA |
|---|---|---|---|---|---|---|---|---|---|---|
| Neptune interior | | | | ■ | ■ | ■ | | | ■ | |
| Neptune atmosphere | ■ | ■ | ■ | | | | ■ | | ■ | ■ |
| Neptune rings and icy satellites | ■ | ■ | ■ | | ■ | ■ | | ■ | | ■ |
| Neptune magnetic environment | | ■ | ■ | | | ■ | | ■ | ■ | |
| Triton interior and surface | ■ | ■ | ■ | ■ | ■ | ■ | ■ | | | ■ |
| Triton atmosphere | ■ | | | | | ■ | | ■ | | ■ |
| Triton-magnetosphere interaction | | ■ | ■ | | | ■ | | ■ | | |
| Cruise science | | | | ■ | ■ | ■ | | ■ | ■ | ■ |

Since plans do not currently exists for multiple 35-m antennas in a single location of the European Tracking Network, an ESA-led mission would require use of the future DSN capability, under a cooperation agreement with NASA.

**Radioisotope Thermoelectric Generators (RTGs) or Stirling Radioisotope Generators (SRGs)**

RTGs are mission enabling technologies for any future mission beyond Jupiter. The European program to develop radioisotope space nuclear power systems is currently at TRL ˜3 [10]. The radioactive isotope chosen for the program is Americium-241, which has a longer half-life than the Plutonium-238 used in conventional RTGs for space exploration. The current European RTG lifetime requirement is 20 years. The lifetime of the RTG units included in this example mission concept is also 20 years, based on a 3-year pre-launch ground phase and 17 years post-launch. Although there are differences between past and present RTG systems and the European units under development, we note that all space RTGs to date have exceeded lifetime requirements (e.g. Cassini-Huygens).

14 European RTGs (10 nominal+4 redundant) are used in this example mission scenario, for a total weight of about 350 kg[10]. 10 RTGs produce a total electric power of 500 W; for comparison, the JPL Neptune orbiter [1] included 2 ASRGs (+1 redundant) for a total power of ˜280 W (100 kg); JUICE uses solar arrays to produce ˜ 640 W at end of life (˜350 kg) [11]. An alternative source of power are the European SRGs, also currently under development [10]; each SRG unit providing twice the power than the European RTGs.

**Solar Electric Propulsion (SEP)**

The RTG lifetime leads to a constraint on the interplanetary transfer time, which can be satisfied using SEP module, an Electric Sail (E-sail)[12], or aerocapture at NOI[1]. SEP is the selected option for this study because of its high TRL; the SEP module is ejected some time before approaching Neptune, and is only used in the earlier part of the interplanetary transfer, where it provides large $\Delta v$'s with a small propellant mass thanks to the high specific impulse. For the same reason, ion engines are preferred to Hall effect thrusters. In this study, four QinetiQ T6 Gridded Ion Engine (3 nominal+1 redundant) are used, each providing 155 mN of thrust and requiring 5.5 kW. These engines have high TRL, as they are implemented on Alphabus, the new European GEO platform launched in 2013, and on BepiColombo. The power for the EP system is provided by the solar arrays; with the current technology, the specific power provided by the power subsystem included in this study is 75 W/kg at 1 AU (Dawn for instance achieved 82 W/kg). The total mass of the SEP module is estimated to be about 1500 kg, including solar arrays (220 kg), tanks (˜70 kg), thrusters (100 kg per engine), propellant (˜700 kg), and structure (˜150 kg). The trade offs between different types of engines, their number, and the size and type of solar arrays, are not relevant for this preliminary discussion, but should be included in future feasibility studies.

**Enhancing technologies**

To focus technology development, a number of enhancing technologies are not included in this example mission concept. "Ultraflex" solar arrays (TRL 6) and ultra-light weight panels[13] are currently under development and will provide larger specific power than the current solar arrays (reaching in theory up to 150-175 W/kg), increasing the available dry mass at Neptune by about 50 kg. An Ariane 5 ME launcher (higher performance, with a restartable upper stage) would not only increase the dry mass at Neptune orbit, but would also decrease the launch cost by around 20%. The qualification flight is scheduled for 2016. Given the low $v_\infty$ at Earth escape, a lunar GA could be introduced a few weeks after launch (following the commissioning phase and a small pericenter burn), increasing the mass at Neptune at the cost of increased complexity. Lunar GAs have already been included in a number of past missions. Further mass savings are obtained when launching the spacecraft into a highly elliptical orbit, and raising the apogee with the onboard engine until escape or a lunar GA; assuming an Ariane 5 launch, however, the savings are marginal (and would not justify the increased complexity of the mission) unless a large propulsion system is used (˜1,500 N )[14].

## 2.3. Gravity losses at Neptune Orbit Insertion (NOI)

At Neptune arrival, the NOI maneuver by the chemical engine places the spacecraft into a closed orbit around Neptune. The required impulsive $\Delta v$ is about 2.5 km/s, however, since the actual maneuver is executed over a finite time interval, mass penalties (gravity losses) will reduce the dry mass delivered into orbit. The gravity losses depend on the impulsive $\Delta v$ (which is large for a Neptune orbit insertion) and on the thrust level of the propulsion system (see appendix for more details). When a single 450 N engine is implemented, the gravity losses for NOI can be as high as 40% in $\Delta v$. Although the design of the chemical propulsion system is outside the scope of this discussion, using high thrust levels is recommended to avoid excessive gravity losses and complex attitude control operations. Examples of large propulsion systems include the MOOG-ISP HTAE of 1100 N (under development), or the three 500 N engines used by the proposed SELENE2 lunar lander.

## 2.4. Mission summary

Table 3 shows an overview of the example mission concept for a Neptune orbiter. This example delivers about two tons of dry mass into Neptune orbit, assuming an impulsive NOI maneuver. Large gravity losses of 40% in $\Delta v$ would result in a mass penalty of ˜500 kg.

*Table 3. Summary. (a)Assuming an impulsive NOI. (b) Includes determistic $\Delta v$ and tour navigation.*

| | |
|---|---|
| Interplanetary mission profile | Launch on 19 Dec 2028 with Ariane 5 ECA.<br>Two Earth Gravity Assists (GA) + 1 Jupiter GA.<br>Transfer time: 15 years.<br>Propulsion: Solar Electric Propulsion (SEP, ejected before Jupiter flyby), total propellant mass of 695 kg. |
| Neptune tour mission profile | Two-year orbital tour (covering all solar local times and a range of orbital inclinations).<br>55 Triton flybys (providing global surface coverage).<br>Propulsion: Chemical, total $\Delta v$ of 3 km/s$^{(a)(b)}$ |
| Power sub-system | 10 European radioisotope thermoelectric generators, providing 500 W at Neptune |
| Mass budget | Mass at launch: 6467 kg<br>SEP module wet mass: 1516 kg<br>Dry mass at Neptune: 1921 kg $^{(a)}$<br>Payload mass: 70 kg |

## 3. Interplanetary transfer to Neptune

Issues such as RTG lifetime (20 years, including pre-launch ground phase) make the duration of an interplanetary transfer to Neptune an essential aspect of any discussion of Neptune orbiter mission concepts. We investigated trajectory options involving a launch from Kourou. Rather than project future Ariane launcher performance, we assume an Ariane 5 ECA launcher for this preliminary analysis. The launcher performances are summarized in the appendix.

The interplanetary transfer to Neptune requires a Gravity Assist (GA) by either Jupiter or Saturn a few years after launch to mitigate propellant requirements. However, a Jupiter GA is more effective than a Saturn GA for a Neptune orbiter mission[6] ; also, useful Saturn-Neptune transfers are not available in the timeframe considered. In general, favorable opportunities for a Jupiter GA will exist in 2033 and in 2046 (separated by a Jupiter-Neptune synodic period of ˜13 years). One or more Earth GAs and orbital maneuvers are also typically required prior to the Jupiter GA. The orbital maneuvers in the first part of the mission can be executed with chemical or electric propulsion; at Neptune arrival, though, the orbit insertion maneuver it is always performed using a chemical propulsion system. It is found that chemical propulsion options would not deliver sufficient mass into Neptune orbit, unless the transfer times is allowed to increase to 16˜17 years; while SEP options would deliver sufficient mass within a transfer time of 15 years.

This section presents several chemical and electric propulsion transfer options. The linked-conic model is used with real ephemerides of the planets, and the final condition of each transfer is a Neptune encounter. A numerically integrated trajectory was also computed, showing that the transfer time is not affected by the linked-conic approximation. At Neptune, the NOI maneuver captures the spacecraft into a 100-day closed orbit. The post-NOI mass for the different scenarios is computed for an impulsive NOI, and include the propellant mass for the pericenter raise maneuver and for the tour navigation (˜500 m/s $\Delta v$).

### 3.1. Chemical propulsion option

A broad search of chemical propulsion options is conducted using SOURCE [7, 8], a dedicated in-house tool based on the linked conics approximation. The tool searches through a variety of transfer types, including resonant transfers and $v_\infty-$leveraging transfers. When SOURCE detects similar solutions, it saves the ones with best performance (highest final mass). For a transfer to Neptune, several sequences of GAs are analyzed with launch between 2025 and 2041. The best performing sequences are:

- Earth - Earth - Venus - Earth - Earth - Jupiter - Neptune
- Earth - Earth - Mars - Earth - Earth - Jupiter - Neptune
- Earth - Earth - Earth - Venus - Earth - Mars - Earth - Jupiter - Neptune
- Earth - Earth - Venus - Earth - Earth - Mars - Jupiter - Neptune
- Earth - Earth - Venus - Venus - Earth - Earth - Jupiter - Neptune
- Earth - Earth - Earth - Jupiter - Neptune

For all the sequences, the spacecraft is initially launched on the Earth equatorial plane into a one-year Earth-to-Earth orbit. The first Earth GA is then used to turn the escape $v_\infty$ in the most suitable direction for the remaining part of the transfer. This strategy is commonly implemented with Earth-escape launches by Ariane 5 ECA, since the launcher performances are strongly penalized at non-zero declinations.

No interesting sequence includes Saturn GA, as the Saturn-Neptune geometry is unfavorable for the period 2025-2040. Some assumptions are used to speed up the global search process. For arcs between the inner planets, only transfers with zero or one complete revolutions are used. For same-planet transfers, $v_\infty-$leveraging maneuvers are included, assuming a maximum leveraging $\Delta v$ of 800 m/s for the Earth, and 200 m/s for Venus. All maneuvers are assumed impulsive and executed with $I_{sp} = 312$ s. The maximum duration of the final arc (Jupiter to Neptune) is assumed to be 3800 days. The post-NOI mass at Neptune is computed assuming an impulsive NOI into a 100-day orbit with a pericenter altitude of 3000 km.

Figure 1 shows the post-NOI mass for launch in 2025-2040. The solutions are clustered around two launch date intervals, which are separated by about one Jupiter-Neptune synodic period. Only very few solutions have a total transfer duration below 17 years and none of them below 16 years. If this finding could trigger future development of RTGs with enhanced lifetime, Fig. 1 also illustrates that final masses of more than 2000 kg can be achieved.

Details of the best solutions from Fig. 1 are provided in Table 4. Three categories for ranking the solutions are used, which is reflected in the nomenclature of the transfer: shortest (S), highest final mass (M), and 'cold' transfers (C). The last category is introduced in case thermal considerations in the spacecraft would not allow to fly by Venus. Figure 2, 3 and 4 show the trajectory plots of some of these options. The first Earth-Earth arc is not included in the plots.

When solutions are optimized enforcing the 15-year constraint, the Jupiter-Neptune arc is reduced, yielding to larger deep space maneuvers and to a higher arrival $v_\infty$ at Neptune. The post-NOI mass would be about 1000kg, much below the required mass for an L-class Neptune orbiter.

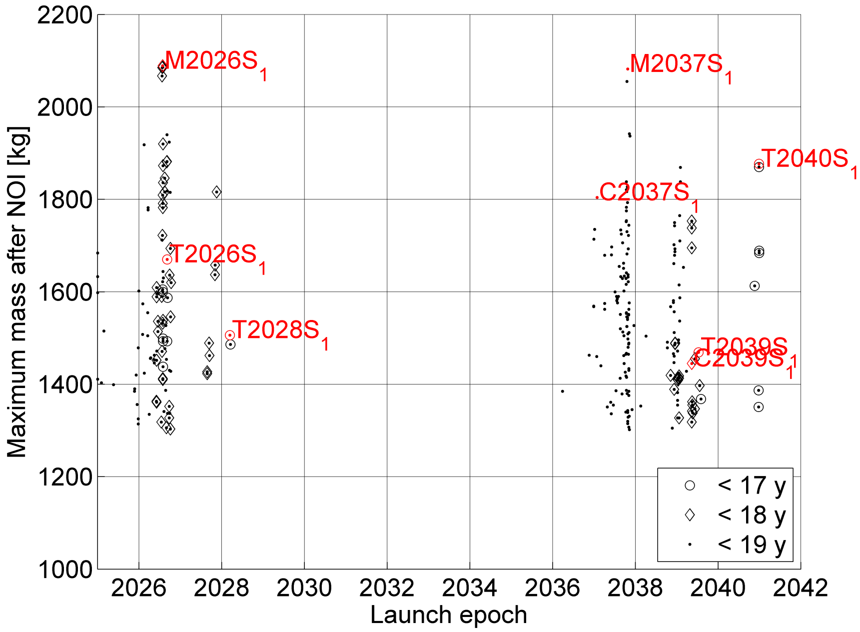


**Figure 1. Mass of chemical transfers after NOI.**

**Table 4. Chemical interplanetary transfer candidates for the period 2025-2041**

| Case | M2026$S_1$ | T2026$S_1$ | T2028$S_1$ | C2037$S_1$ | M2037$S_1$ | C2039$S_1$ | T2039$S_1$ | T2040$S_1$ |
|---|---|---|---|---|---|---|---|---|
| Launch date | (E) 25/07/29 | (E) 25/09/07 | (E) 27/03/13 | (E) 36/01/28 | (E) 36/10/26 | (E) 38/05/13 | (E) 38/07/13 | (E) 39/12/28 |
| Launch V-infinity (km/s) | 2.94 | 3.41 | 3.44 | 3.09 | 3.07 | 3.54 | 4.09 | 3.1 |
| Launch mass (kg) | 5027 | 4560 | 4537 | 4877 | 4901 | 4434 | 3862 | 4872 |
| Swing-by date | (E) 26/07/29 | (E) 26/09/07 | (E) 28/03/13 | (E) 37/01/28 | (E) 37/10/26 | (E) 39/05/13 | (E) 39/07/13 | (E) 40/12/28 |
| Swing-by date | (V) 26/11/20 | (V) 27/02/22 | (V) 28/07/07 | (M) 39/07/03 | (V) 38/04/14 | (M) 41/10/09 | (V) 40/01/01 | (V) 41/04/21 |
| DSM (m/s) | 0 | 0 | 0 | 110 | 0 | 840 | 0 | 0 |
| Swing-by date | (E) 28/03/04 | (E) 27/12/28 | (E) 30/03/24 | (E) 40/12/03 | (V) 40/01/12 | (E) 42/02/25 | (E) 41/06/04 | (E) 42/01/17 |
| DSM (m/s) | 0 | 0 | 330 | 20 | 0 | 0 | 20 | 330 |
| Swing-by date | (E) 31/03/05 | (E) 29/12/28 | (E) 32/03/11 | (E) 43/03/05 | (E) 42/01/04 | (E) 44/02/25 | (E) 43/01/17 | (E) 44/04/15 |
| DSM (m/s) | 0 | 0 | 640 | 10 | 0 | 0 | 10 | 0 |
| Swing-by date | (M) 31/05/20 | - | - | - | (E) 44/04/13 | - | - | - |
| DSM (m/s) | 20 | 0 | 0 | 0 | 50 | 0 | 0 | 0 |
| Swing-by date | (J) 32/12/05 | (J) 32/01/02 | (J) 33/08/30 | (J) 45/02/07 | (J) 45/11/25 | (J) 45/11/17 | (J) 45/01/28 | (J) 45/11/25 |
| DSM (m/s) | 0 | 10 | 0 | 0 | 0 | 10 | 10 | 10 |
| Arrival date | (N) 43/05/02 | (N) 42/05/26 | (N) 44/01/24 | (N) 55/07/03 | (N) 56/04/20 | (N) 56/04/13 | (N) 55/06/24 | (N) 56/04/20 |
| Arrival $v_\infty$(km/s) | 11.1 | 11.9 | 10.4 | 11.6 | 10.8 | 10.9 | 11.6 | 10.8 |
| NOI (m/s) | 2670 | 3060 | 2400 | 2900 | 2570 | 2580 | 2910 | 2570 |
| Total $\Delta v$(m/s) | 2686 | 3074 | 3375 | 3043 | 2619 | 3430 | 2957 | 2917 |
| Final mass (kg) | 2089 | 1670 | 1506 | 1804 | 2082 | 1445 | 1469 | 1877 |
| Duration (year) | 17.8 | 16.7 | 16.9 | 19.4 | 20.5 | 17.9 | 16.9 | 16.3 |
| Legend | (V)enus | (E)arth | (M)ars | (J)upiter | (N)eptune | | | |

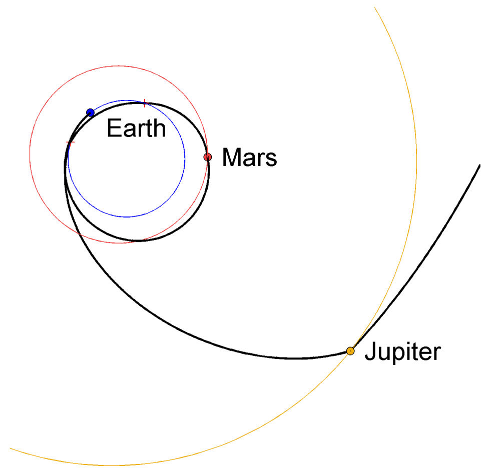


**Figure 2. Ecliptic projection of solution C2037S$_1$. It is based on a MEEJ sequence.**

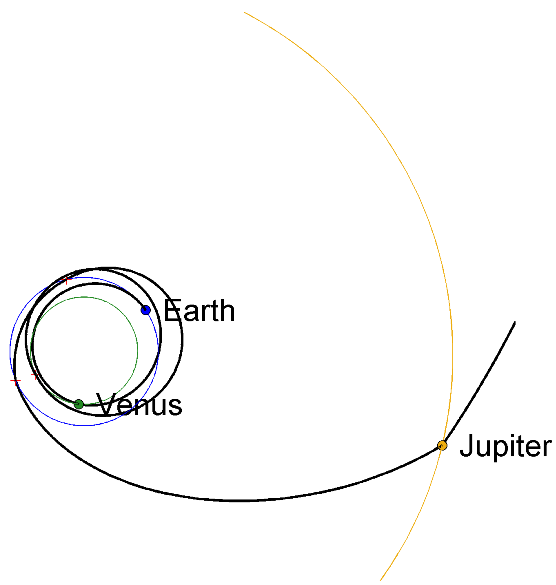


**Figure 3. Ecliptic projection of solution M2037S$_1$. It is based on a VVEEJ sequence.**

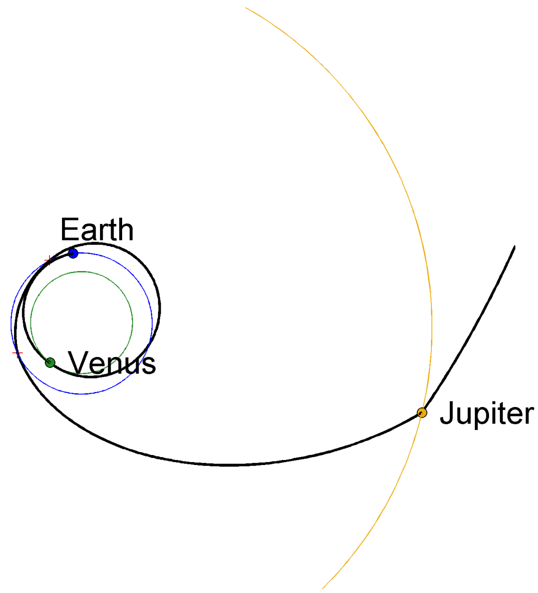


**Figure 4. Ecliptic projection of solution T2040S$_1$. It is based on a VEEJ sequence.**

### 3.2. Solar electric propulsion option

Some examples of electric propulsion trajectories to Neptune are available in literature. Yam et al.[5] computed nuclear electric propulsion options; Landau et al.[6] computed several SEP trajectories to Neptune with a 13-year time of flight, AltasV(551) launch, and NEXT engines. In this section we present two example SEP trajectories with an Ariane 5 ECA launch (which requires a 1:1 Earth resonant orbit), and three ion engines for a total thrust of 0.465 N (maximum, at 1 AU). Figure 5 shows the transfer used for the example mission concept, and Figure 6 shows another example with launch in 2041. The transfers are similar and include flybys at Earth and Jupiter only. Low-thrust arcs are modeled with small impulsive maneuvers, which are represented as arrows. Table 5 shows the summary of the SEP trajectoy with launch in 2028.

*Table 5. Summary of the SEP trajecory. (a) Includes the SEP module. (b) Assuming an impulsive NOI.*

| ***Event*** | ***Epoch*** | ***Mass (kg)*** | $v_\infty$***(km/s)*** |
|---|---|---|---|
| Launch | 2028 DEC 19 | 6467 | 0.76 |
| Earth GA1 | 2030 FEB 21 | 6102 | 4.83 |
| Earth GA2 | 2032 APR 13 | 5817 | 10.46 |
| Jupiter GA | 2033 SEP 03 | 5772 | 11.73 |
| Neptune arrival | 2043 DEC 20 | 5772$^{(a)}$ | 10.56 |
| *Post-NOI* | | *2267*$^{(b)}$ | |

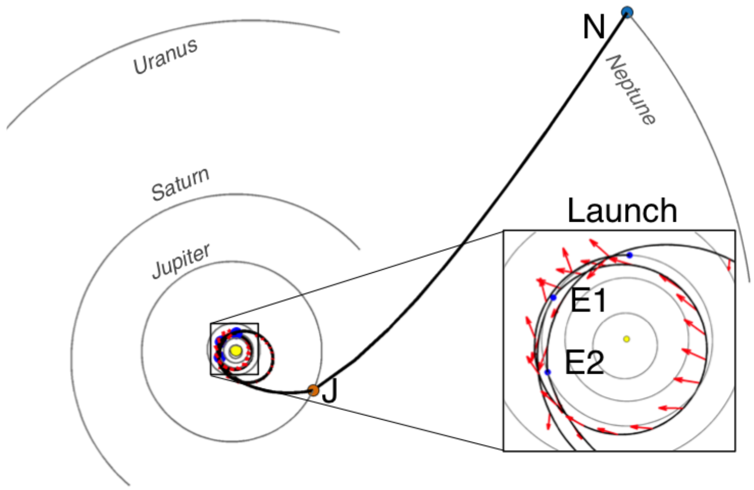


**Figure 5. An example interplanetary transfer with launch in 2028**

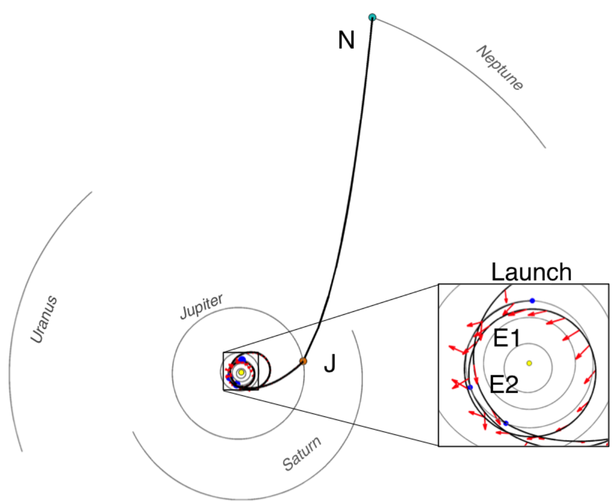


**Figure 6. An example interplanetary transfer with launch in 2041**

## 4. Neptune orbital tour

This section presents an example two-year tour covering a wide range of Neptune orbits and Triton flyby geometries. Although not included here, close flybys at other moons and opportunities for Neptune or Triton occultation can be added.

The tour is computed using linked-conics approximation and Triton ephemerides; Figure 7 shows the trajectory in the inertial frame, and Table 6 summarizes the tour events. The spacecraft flies inside the inner rings and executes NOI; at the first apocenter, a Pericenter Raise Maneuver (PRM) raises the pericenter outside the rings and targets the first Triton flyby T1. Starting with T1, a first sequence of flybys (called Crank-Over-the-Top sequence[15]) increases the inclination of the spacecraft orbit over Neptune's equatorial plane.

Table 6. Tour events.

| *Event* | *Epoch* | Δ*v (km/s)* | | | | | | |
|---|---|---|---|---|---|---|---|---|
| NOI | 2044 DEC 20 | 2.45 | | | | | | |
| PRM | 2044 FEB 12 | 0.29 | | | | | | |
| ***Event*** | ***Epoch*** | $v_{\infty in}$ ***(km/s)*** | | | $v_{\infty ou}$ ***(km/s)*** | | | ***h (km)*** |
| T1 | 2044 APR 02 | 2.80 | 0.87 | -0.50 | 2.91 | 0.52 | -0.39 | 1000 |
| T2 | 2044 MAY 08 | 2.91 | 0.52 | -0.39 | 2.97 | 0.13 | -0.12 | 500 |
| T3 | 2044 MAY 25 | 2.97 | 0.13 | -0.12 | 2.95 | -0.20 | 0.31 | 250 |
| T4 | 2044 JUN 06 | 2.95 | -0.20 | 0.31 | 2.84 | -0.49 | 0.75 | 250 |
| T5 | 2044 JUN 24 | 2.84 | -0.49 | 0.75 | 2.68 | -1.01 | 0.80 | 250 |
| T6 | 2044 JUN 30 | 2.68 | -1.01 | 0.80 | 2.48 | -1.01 | 1.30 | 250 |
| T7 | 2044 JUL 05 | 2.48 | -1.01 | 1.30 | 2.18 | -1.01 | 1.76 | 250 |
| T8 | 2044 JUL 11 | 2.18 | -1.01 | 1.76 | 1.90 | -1.47 | 1.76 | 250 |
| T9 | 2044 JUL 29 | 1.90 | -1.47 | 1.76 | 1.57 | -1.90 | 1.67 | 250 |
| T10 | 2044 AUG 16 | 1.57 | -1.90 | 1.67 | 1.22 | -2.30 | 1.45 | 150 |
| T11 | 2044 AUG 21 | 1.22 | -2.30 | 1.45 | 0.76 | -2.30 | 1.73 | 250 |
| T12 | 2044 AUG 27 | 0.76 | -2.30 | 1.73 | 0.54 | -2.00 | 2.14 | 250 |
| T13 | 2044 SEP 20 | 0.54 | -2.00 | 2.14 | 0.97 | -1.69 | 2.25 | 250 |
| T14 | 2044 OCT 02 | 0.97 | -1.69 | 2.25 | 1.46 | -1.47 | 2.14 | 250 |
| T15 | 2044 OCT 19 | 1.46 | -1.47 | 2.14 | 1.73 | -1.01 | 2.20 | 250 |
| T16 | 2044 OCT 25 | 1.73 | -1.01 | 2.20 | 2.13 | -1.01 | 1.82 | 250 |
| T17 | 2044 OCT 31 | 2.13 | -1.01 | 1.82 | 2.44 | -1.01 | 1.38 | 250 |
| T18 | 2044 NOV 06 | 2.44 | -1.01 | 1.38 | 2.66 | -1.01 | 0.88 | 250 |
| T19 | 2044 NOV 12 | 2.66 | -1.01 | 0.88 | 2.78 | -1.01 | 0.35 | 250 |
| T20 | 2044 NOV 18 | 2.78 | -1.01 | 0.35 | 2.92 | -0.49 | 0.28 | 250 |
| T21 | 2044 DEC 05 | 2.92 | -0.49 | 0.28 | 2.96 | -0.35 | -0.00 | 1510 |
| T22 | 2044 DEC 14 | -2.96 | -0.35 | 0.00 | -2.98 | -0.09 | -0.00 | 2149 |
| T23 | 2044 DEC 28 | 2.98 | -0.09 | 0.00 | 2.96 | -0.35 | -0.00 | 2149 |
| T24 | 2045 JAN 06 | -2.96 | -0.35 | 0.00 | -2.98 | -0.09 | -0.00 | 2149 |
| T25 | 2045 JAN 21 | 2.98 | -0.09 | 0.00 | 2.96 | -0.35 | -0.00 | 2149 |
| T26 | 2045 JAN 29 | -2.96 | -0.35 | 0.00 | -2.98 | -0.09 | -0.00 | 2149 |
| T27 | 2045 FEB 13 | 2.98 | -0.09 | 0.00 | 2.96 | -0.35 | -0.00 | 2149 |
| T28 | 2045 FEB 21 | -2.96 | -0.35 | 0.00 | -2.98 | -0.09 | -0.00 | 2149 |
| T29 | 2045 MAR 08 | 2.98 | -0.09 | 0.00 | 2.96 | -0.35 | -0.00 | 2149 |
| T30 | 2045 MAR 16 | -2.96 | -0.35 | 0.00 | -2.97 | 0.18 | -0.00 | 293 |
| T31 | 2045 APR 06 | 2.97 | 0.18 | -0.00 | 2.96 | -0.35 | 0.00 | 294 |
| T32 | 2045 APR 14 | -2.96 | -0.35 | -0.00 | -2.97 | 0.18 | -0.00 | 293 |
| T33 | 2045 MAY 04 | 2.97 | 0.18 | 0.00 | 2.96 | -0.35 | 0.00 | 294 |
| T34 | 2045 MAY 13 | -2.96 | -0.35 | -0.00 | -2.97 | 0.18 | -0.00 | 293 |
| T35 | 2045 JUN 02 | 2.97 | 0.18 | 0.00 | 2.95 | -0.20 | -0.39 | 250 |
| T36 | 2045 JUN 14 | 2.95 | -0.20 | -0.39 | 2.82 | -0.49 | -0.83 | 250 |
| T37 | 2045 JUL 01 | 2.82 | -0.49 | -0.83 | 2.66 | -1.01 | -0.87 | 250 |
| T38 | 2045 JUL 07 | 2.66 | -1.01 | -0.87 | 2.44 | -1.01 | -1.37 | 250 |
| T39 | 2045 JUL 13 | 2.44 | -1.01 | -1.37 | 2.13 | -1.01 | -1.82 | 250 |
| T40 | 2045 JUL 19 | 2.13 | -1.01 | -1.82 | 1.85 | -1.47 | -1.81 | 250 |
| T41 | 2045 AUG 06 | 1.85 | -1.47 | -1.81 | 1.52 | -1.90 | -1.71 | 250 |
| T42 | 2045 AUG 23 | 1.52 | -1.90 | -1.71 | 1.18 | -2.30 | -1.48 | 150 |
| T43 | 2045 AUG 29 | 1.18 | -2.30 | -1.48 | 0.71 | -2.30 | -1.75 | 250 |
| T44 | 2045 SEP 04 | 0.71 | -2.30 | -1.75 | 0.18 | -2.30 | -1.88 | 250 |
| T45 | 2045 SEP 10 | 0.18 | -2.30 | -1.88 | 0.09 | -1.90 | -2.29 | 150 |
| T46 | 2045 SEP 28 | 0.09 | -1.90 | -2.29 | -0.07 | -1.47 | -2.59 | 250 |
| T47 | 2045 OCT 15 | -0.07 | -1.47 | -2.59 | -0.27 | -1.01 | -2.79 | 250 |
| T48 | 2045 OCT 21 | -0.27 | -1.01 | -2.79 | -0.80 | -1.01 | -2.68 | 250 |
| T49 | 2045 OCT 27 | -0.80 | -1.01 | -2.68 | -1.31 | -1.01 | -2.48 | 250 |
| T50 | 2045 NOV 02 | -1.31 | -1.01 | -2.48 | -1.76 | -1.01 | -2.18 | 250 |
| T51 | 2045 NOV 08 | -1.76 | -1.01 | -2.18 | -2.15 | -1.01 | -1.80 | 250 |
| T52 | 2045 NOV 14 | -2.15 | -1.01 | -1.80 | -2.46 | -1.01 | -1.35 | 250 |
| T53 | 2045 NOV 19 | -2.46 | -1.01 | -1.35 | -2.67 | -1.01 | -0.85 | 250 |
| T54 | 2045 NOV 25 | -2.67 | -1.01 | -0.85 | -2.82 | -0.49 | -0.80 | 250 |
| T55 | 2045 DEC 13 | -2.82 | -0.49 | -0.80 | -2.95 | -0.20 | -0.36 | 250 |

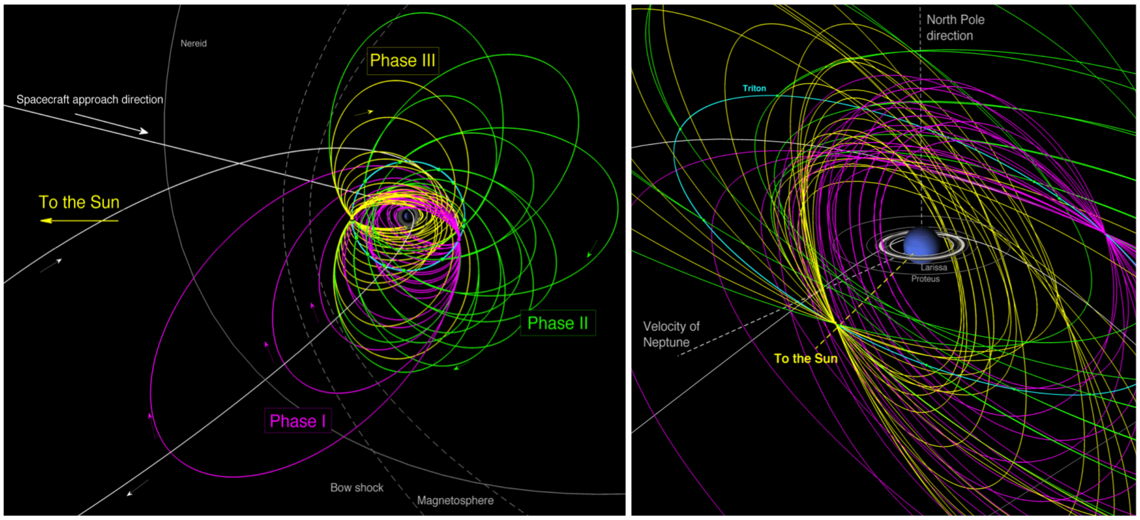

Figure 7. Example two-year tour. (A) Viewed from Neptune's north pole. (B) Close-up of the tour.

The design of the initial part of the tour (up to T1) involves several trade-offs. The period of the first orbit is 100 days , since longer periods do not significantly reduce the NOI $\Delta v$. The pericenter altitude should be as low as possible, and it is assumed to be at 3,000 km altitude (following previous NASA mission concepts [1]). The location of T1 should be close to the line of nodes between the orbital plane of Triton and Neptune's equator, to maximize the inclination that be achieved with the COT sequence. At the same time, T1 should be close to the Sun-Neptune direction, to maximize the lighting conditions of the groundtracks of the COT flybys. Finally, a high $v_\infty$ at T1 maximizes the inclination achievable with the COT, while a low $v_\infty$ maximizes the bending angle of each flyby, and hence the number of flybys and the total tour duration; for this example tour, we choose a $v_\infty$ of ˜ 3 km.

The rest of the tour has no deterministic orbital maneuvers and is split into three phases. Phase I consists of the first COT sequence, with 20 Triton flybys (altitudes between ˜150 and ˜1,000 km) at the same Triton orbital location. The initial flybys have high altitudes to cope with the larger uncertainties in Triton's ephemerides. Neptune orbits in this phase range in inclination ($115^\circ - 160^\circ$), pericenter radius (75,000-250,000 km), and solar local time (2 PM - 11 PM at apocenter). Figure 8 shows the flybys of Phase I with the nadir-pointing groundtracks of the 20 flybys, which are concentrated on the sunlit Neptune-facing hemisphere.

During Phase II, the spacecraft orbit lies in Triton's orbital plane. 14 flybys rotate the line of apsides in the anti-clockwise direction using the "petal strategy" technique, which alternates long and short non-resonant transfers[16, 15]. In this phase the apocenter varies between 800,000-1,300,000 km altitude and between 2 PM - 5 AM solar local times. The flyby groundtracks are equatorial, centered alternately at $0^\circ$ and $180^\circ$ Triton longitude, with minimum altitudes between 300 and 2,000 km. Flybys occur all along Triton's orbit at $\sim 30^\circ$ degree intervals. The last flyby of this phase lies on the opposite side of Triton's orbit compared to the first flyby, close to the orbital node to maximize the achievable inclination of the following phase.

Phase III consists of a second COT sequence with 21 Triton flybys. Neptune orbits are once

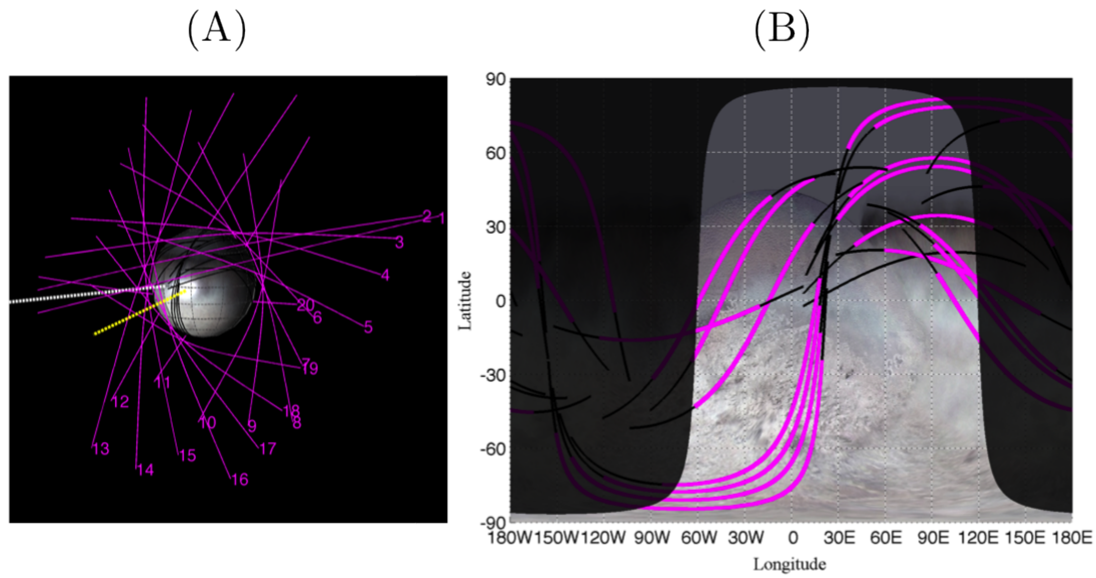


Figure 8. Flybys at Triton during Phase I (A), and corresponding groundtracks (thin lines: below 5000 km altitude; thick lines: below 1000 km altitude)(B)

again varied in inclination ($115^\circ - 160^\circ$) and solar local time (7 AM - 5 PM at apocenter). The groundtracks are concentrated in the sunlit anti-Neptune-facing hemisphere, as shown in Fig. 9.

The tour is designed using the $v_\infty$- sphere[17], and the formulas that connect multiple flybys with resonant orbits. In particular, we use the formulation developed in [18], but similar formulas are found for example in [17, 19]. Figure 10 shows the Triton tour on the $v_\infty$- sphere, parametrized by the pump and crank angles. Each point corresponds to an orbit; the vertical lines are resonant orbits. The shaded regions are orbits that collide with Neptune or its rings.

For the tour, $\Delta v$˜250 m/s is allocated for navigation: ˜ 3m/s per flyby with the exception of the first 10 flybys, where ˜ 10 m/s are allocated for the initial large uncertainties on Triton ephemerides. For the same reason, the altitude of the first flyby is kept at 1000 km, and the altitude of the second flyby is 500 km, while for most of the following flybys, the minimum altitude is 250 km. At 250 km, the dynamic pressure (hence heat loads and controllability) is similar to that experienced by Cassini during the Titan flybys. The flybys T10, T45, and T45 are examples of lower altitude flybys (150 km), where the dynamic pressure is similar to that of a 750/800-km altitude flyby at Titan with $v_\infty$ ˜6 km/s (Cassini lowest-altitude flyby was at 880 km, T70). The altitude of these flybys can be increased with a marginal penalty in the tour duration.

Although not included here, a Triton orbit phase could also be considered at the end of the Neptune tour, or replacing part of it, at the additional cost of $\Delta v$˜300 m/s. Over the course of 3-4 months a sequence of high-altitude Triton flybys and orbital maneuvers would reduce the spacecraft velocity relative to Triton, eventually leading to a gravitational capture orbit that is stabilized by a Triton orbit insertion maneuver[20]. This type of transfer was used for the lunar orbit insertion of the SMART1 spacecraft, and is planned for JUICE Ganymede orbit insertion to reduce the required propellant mass.

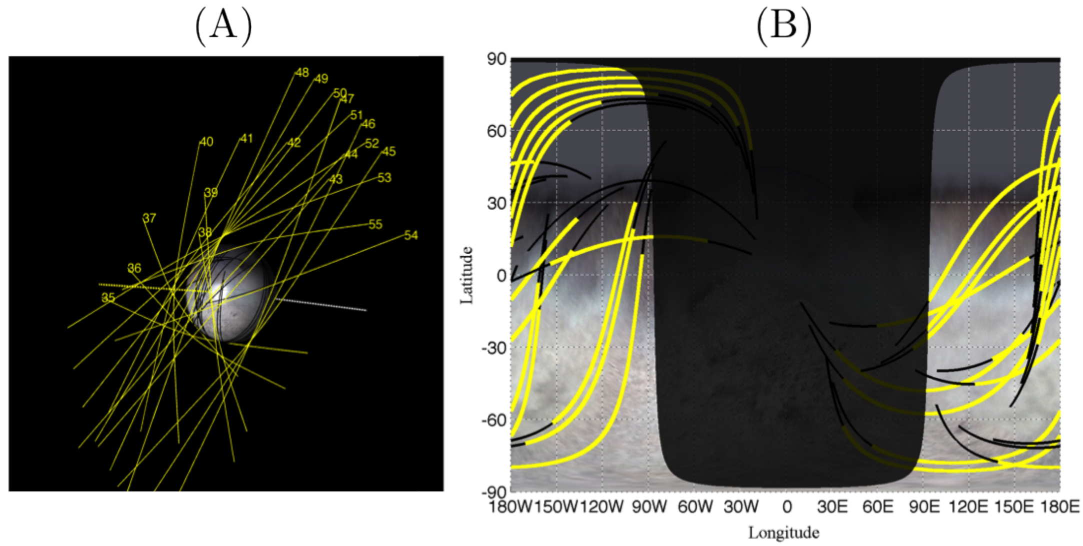


Figure 9. Flybys at Triton during Phase III (A), and corresponding groundtracks (thin lines: below 5000 km altitude; thick lines: below 1000 km altitude)(B)

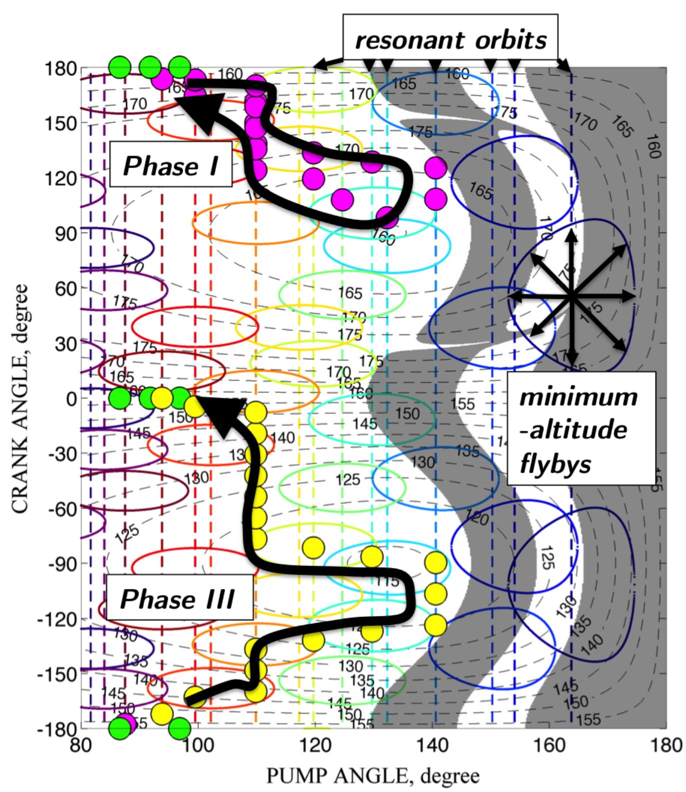


**Figure 10. Design of the tour on the $v_\infty$ sphere.**

## 5. Acknowledgments

SC would like to thank several colleagues for their useful input: Maite Arza, Carlos Corral van Damme, Yasuhiro Kawakatsu, Michael Khan, Damon Landau, Markus Landgraf, Jean-Pierre Lebreton, Nathan Strange. AM and SC acknowledge the support of the JAXA International Top Young Fellowship Program.

## APPENDIX

### Ariane 5 ECA performances

For the calculation of the escape mass, the updated Ariane 5 ECA performance are used (see Table 7). These figures include an adapter mass of 155 kg.

Table 7. Updated performance of the Ariane 5 ECA for an escape declination of 0°. This performance is actually an extrapolation of what is given in [21], for which 3 cases have been analyzed: 3.05, 3.15 and 3.38 km/s

| $v_\infty$ [km/s] | escape mass [kg] |
|---|---|
| 0.5 | 6686 |
| 1.0 | 6544 |
| 1.5 | 6312 |
| 2.0 | 5993 |
| 2.5 | 5594 |
| 3.0 | 5124 |
| 3.5 | 4629 |
| 4.0 | 4113 |
| 4.5 | 3568 |
| 5.0 | 3008 |
| 5.5 | 2441 |

### Gravity losses at NOI

Chemical propulsion is needed for the NOI. The arrival infinite velocity at Neptune is essentially fixed by the constraint on the maximum transfer time between Jupiter and Neptune; its value usually lies between 10 km/s and 12 km/s. Parametric analyses were performed by varying the arrival infinite velocity and the main engine thrust for which two values were considered: 450 N and 900 N, the latter either representing two 450 N engines or a bigger engine. These analyses are summarized in Table 8.

Table 8. NOI as a function of the incoming infinite velocity and the engine thrust. The pericenter altitude of the orbit after capture is 3000 km and the period is 100 days. The initial mass is 4 tons.

| Case | $v_\infty$ [km/s] | $F$ [N] | $\Delta v$ [km/s] | $\Delta v$ g.l. [%] | $\Delta t$ [hour] | $\Delta m$ [kg] | $m_f$ [kg] | $\Delta m$ g.l. [%] |
|---|---|---|---|---|---|---|---|---|
| 1 | 10 | 450 | 3.04 | 37.5 | 4.8 | 2506 | 1494 | 22.5 |
| 2 | 11 | 450 | 3.65 | 38.2 | 5.3 | 2772 | 1228 | 20.6 |
| 3 | 12 | 450 | 4.27 | 37.9 | 5.7 | 2996 | 1004 | 18.3 |
| 4 | 10 | 900 | 2.63 | 18.9 | 2.2 | 2293 | 1707 | 12.1 |
| 5 | 11 | 900 | 3.18 | 20.6 | 2.5 | 2572 | 1428 | 12.0 |
| 6 | 12 | 900 | 3.77 | 21.5 | 2.7 | 2818 | 1182 | 11.3 |

By comparing Case 1 to 3, it can be observed that the infinite velocity magnitude plays a minor role on the $\Delta v$ gravity losses, which remain around 38 %. The propellant mass gravity losses are around 20 %, i.e. around 470 kg into capture orbit. This figure has to be compared with the spacecraft dry mass (around 1500 kg). By comparing Case 1 to Case 4, 2 to 5 or 3 to 6, it can be observed that gravity losses are roughly divided by a factor 2 when the engine thrust is multiplied by 2. This also applies to the duration of the maneuver, for which standard engines are usually qualified for a couple of hours of consecutive activation. From these observations it is clear that a minimum thrust of around 1000 N is needed in order to keep propellant gravity losses below 10 % and to be compliant with the engine qualification domain.

## 6. References


[1] Marley, M., Dudzinski, L., Spilker, T., and Moeller, R. "Planetary Science Decadal Survey JPL Rapid Mission Architecture Neptune-Triton-KBO Study Final Report." 2010.

[2] Christophe, B., Spilker, L., and Anderson, J. "OSS (Outer Solar System): a fundamental and planetary physics mission to Neptune, Triton and the Kuiper Belt." Experimental Astronomy, Vol. 34, No. 203, 2012.

[3] Ingersoll, A. and Spilker, T. R. "A Neptune Orbiter with Probes Mission with Aerocapture Orbit Insertion." "Progress in Astronautics and Aeronautics: NASA Space Science Vision Missions, 224," pp. 81–113. AIAA, Reston, VA, 2008.

[4] Pessina, S. M., Campagnola, S., and Vasile, M. "Preliminary Analysis of Interplanetary Trajectories with Aerogravity and Gravity Assist Manoeuvres." "54th International Astronautical Congress," October. 2003.

[5] Yam, C. H. and McConaghy, T. T. "Design of low-thrust gravity-assist trajectories to the outer planets." 55th International Astronautical Congress, 2004.

[6] Landau, D. F., Lam, T., and Strange, N. J. "Broad Search and Optimization of Solar Electric Propulsion Trajectories to Uranus and Neptune." Advances in the Astronautical Sciences, Vol. 153, No. 3, pp. 2093–2112, 2009.

[7] Boutonnet, A., Martens, W., and Schoenmaekers, J. "SOURCE: A Matlab-oriented Tool for Interplanetary Trajectory Global Optimization, Fundamentals (Part I)." Paper AAS 13-300, AAS/AIAA SFMM. Kauai (HA), USA.

[8] Martens, W., Boutonnet, A., and Schoenmaekers, J. "SOURCE: A Matlab-oriented Tool for Interplanetary Trajectory Global Optimization, Applications (Part II)." Paper AAS 13-301, AAS/AIAA SFMM. Kauai (HA), USA.

[9] Masters, A., Achilleos, N., Agnor, C., Campagnola, S., Charnoz, S., Christophe, B., Coates, A., Fletcher, L., Jones, G., Lamy, L., Marzari, F., Nettelmann, N., Ruiz, J., Ambrosi, R., Andre, N., Bhardwaj, A., Fortney, J., Hansen, C., Helled, R., Moragas-Klostermeyer, G., Orton, G., Ray, L., Reynaud, S., Sergis, N., Srama, R., and Volwerk, M. "Neptune and Triton : Essential Pieces of the Solar System puzzle." Planetary and Space Science (submitted), 2014.

[10] Ambrosi, R., Williams, H., Samara-Ratna, P., Jorden, A., Slade, R. M., Jaegle, M., Koenig, J., Bannister, N., Deacon, T., Stuttard, M., Crawford, E., and Vernon, D. "Thermoelectric Converter System for Small-Scale RTGs." Tech. rep., ESA TRP Report, TECS-RTG-TR-D8-001-UL, 2012.

[11] Dougherty, M. "JUICE: exploring the emergence of habitable worlds around gas giants, Assessment Study Report." Tech. rep., ESA/SRE(2011)18., 2011.

[12] Janhunen, P., Quarta, A. A., and Mengali, G. "Electric solar wind sail mass budget model." Geoscientific Instrumentation, Methods and Data Systems Discussions, Vol. 2.2, pp. 429,455, 2013.

[13] Shimazaki, K., Takahashi, M., Imaizumi, M., and Al., E. "First Approach to Lightweight Solar Panel using Space Solar Sheet,." "Proceedings of 8th European Space Power Conference," 2008.

[14] Khan, M. "Summary of Generic Results on Jupiter Orbit Insertion." ESA/ESOC, MAS-TN-058, Sep. 2006.

[15] Buffington, B. B., Strange, N. J., and Campagnola, S. "Global moon coverage via hyperbolic flybys." 23rd International Symposium on Space Flight Dynamics, 2012.

[16] Anderson, R. L., Campagnola, S., and Buffington, B. B. "Analysis of Petal Rotation Trajectory Characteristics." "Astrodynamics Specialist Conference," 2014.

[17] Strange, N. J., Russell, R. P., and Buffington, B. B. "Mapping the V-Infinity Globe." "AAS/AIAA Astrodynamics Specialist Conference and Exhibit, Mackinac Island, MI," 2007.

[18] Campagnola, S. and Kawakatsu, Y. "3D resonant hopping strategies and the Jupiter Magnetospheric Orbiter." Journal of Guidance, Control, and Dynamics, Vol. 35, No. 1, pp. 340–344, 2012. doi:10.2514/1.53334.

[19] Kawakatsu, Y. "V-infinity Direction Diagram and its Application to Swingby Design." "Proceedings of the 21st International Symposium on Space Flight Dynamics," 1. Toulouse, France, 2009.

[20] Campagnola, S., Boutonnet, A., Schoenmaekers, J., Grebow, D. J., Petropoulos, A. E., and Russell, R. P. "Tisserand-Leveraging Transfers." Journal of Guidance, Control, and Dynamics, pp. 1–9, Mar. 2014. ISSN 0731-5090. doi:10.2514/1.62369.

[21] Lux, A. "Feasibility Mission Analysis - Trajectory and Performance Study Laplace Mission on Ariane-5-ECA. Report AE-NT-1-H-049-AE; March 2006; Issue 1; Rev. 0."